PERFORMANCE EVALUATION OF A SALINITY-GRADIENT SOLAR POND MODEL UNDER EGYPTIAN SOLAR RADIATION CONDITIONS

Wessam E. Abd Allah[*], M. K. Abd El-Wahab, M. M. A. El-Sharabasy and M. M. Ali

Agric. Eng. Dept., Fac. Agric., Zagazig Univ., Egypt

ABSTRACT

A salinity gradient solar pond (SGSP), termed in this work "solar pond", is a simple and effective way of capturing and storing solar energy. This paper presents the results of temperature developed in the inner zones of a salinity gradient solar pond model (SGSPM) under Egyptian solar radiation climate conditions during 2010. An insulated solar pond model with a surface area of 1.5 m × 1.5 m and a depth of 1.44 m was constructed at Faculty of Agriculture, Zagazig University, Sharkia Governorate, Egypt (Latitude 30° 35/N, Longitude 31° 31/E). SGSPM filled with prepared different concentrations of sodium chloride salt in water of densities to form salty water zones (upper convective zone, UCZ, the non-convective zone, NCZ, and the lower convective zone, LCZ, with thickness of 0.1, 0.6 and 0.74 m, respectively). The salinity difference between UCZ and LCZ was 6% for 1st experiment, 10% for 2nd experiment and 15 % for 3rd experiment. Twelve temperature sensors (thermocouples type "T") were distributed vertically at different locations along the centered inner zones of the pond to measure temperature variations during day times. Temperature difference was an important indicator for forced heat transfer. The highest stored temperature was obtained from 3rd experiment as follow: 38.3, 49.9 and 53.5°C for UCZ, NCZ and LCZ, respectively in April; 39.1, 52.6 and 58.8°C in June; 24.7, 31.8 and 37.9°C in December. A mathematical analysis was conducted to calculate the efficiency of the solar pond in collecting solar energy. It is noticed that, the collection efficiency of the solar pond was about 29.2% by SGSPM with a depth of 1.44 m under Egyptian climate conditions.

Keywords: Solar pond, energy storage, collecting solar energy, thermal efficiency, salt gradient.

INTRODUCTION

Solar pond is simply a pool of water which collects and stores solar energy, or it is a body of water containing brackish (highly saline) water that forms layers of differing salinity (stratifies) that absorb and trap solar energy. It can be used to provide heat for industrial or agricultural processes, building heating and cooling, water desalination, refrigeration, drying and to generate electricity.

It is a captor of solar energy, able to store and keep heat accumulated for extended periods, whose concentration increases with depth, going from a rather low value on the surface to a value close to saturation in depth. A solar pond consists of three layers of water with a different saline gradient: the Upper Convective Zone (UCZ), the Non-Convective Zone (NCZ) and the Lower Convective Zone (LCZ). The LCZ acts as a collector and storage area, the UCZ ears all the environmental influences while the NCZ called the gradient zone acts as an insulator to limit double-diffusion of heat and salt from the LCZ to the UCZ. When a ray of solar radiation is incident at the air–water interface of a solar pond, part of the ray is reflected back into air while the remaining part is transmitted into the pond. This latter part must pass through one or more meters of water and reach the LCZ to provide useful heat. If the concentration gradient of the NCZ is great enough, no convective motion will occur in this region. The energy absorbed in the bottom of the pond

[*] Corresponding author: Tel. : +201092948019
E-mail address: dr.wesam15@yahoo.com

will be stored in the LCZ. When the temperature of the LCZ reaches a critical value, a convective motion appears. This motion increases in time and leads to the destruction of the interface between the LCZ and the NCZ. As a result, the storage process is adversely affected. Kurt et al. (2000), Jaefarzadeh (2004) and Karakilcik et al. (2006) mentioned that, the efficiency of a solar pond in collecting energy depends on the stability of the gradient zone. Maintaining the state of the salt gradient zone (boundaries, level and salt gradient of NCZ) as her initial design is essential to the successful operation of a salinity gradient solar pond. Both of the upper and lower zones cause erosion of the boundaries of the salt gradient zone. The progress of erosion leads to the reduction of thickness of the NCZ; thus the pond gets destroyed, whether care is not taken. Angeli and Leonardi (2004) observed during the winter period, when typical solar radiation of about 140 W/m^2 (at 39 °N) is available, and UCZ and LCZ temperatures are about 10 and 70°C, respectively. In this case, if a solar pond is constructed to maximize the solar energy capture during the summer (when the LCZ temperature can easily reach about 90°C and therefore, the NCZ thickness is of about 2.5 m), in winter a heat storage efficiency of about 26 % should be attained, which is about 4 % less than it's maximum obtainable value, which should correspond to a NCZ thickness of about 4 m). Akbarzadeh et al. (2005) mentioned that, the temperature difference created between the top and the bottom of the solar ponds can be as high as 50–60°C. Dah et al. (2005) studied experimentally the evolution of the temperature and salinity profiles in a salinity gradient solar pond using a small model pond with 1 m height, 0.9 m diameter. The tank was insulated by 150 mm of polyurethane. Solar radiation was simulated by a 2000 W light projector that presents a spectrum similar to the solar one. The measurements were taken during a period of 29 days of experimentation. The temperature profile was established in the small model pond after 5 days of heating. The maximum temperature attained in the storage zone was 45 °C carrying out a difference in temperature between the bottom and the surface of the pond of 23 °C when the projector is put off and 17 °C when it is put on. Karakilcik et al. (2006) investigated a solar pond with surface area dimensions of 2×2 m, and a

depth of 1.5 m. The salt-water solution is prepared by dissolving the NaCl reagent into fresh water. The thicknesses of the UCZ, NCZ and HSZ were 0.1, 0.6 and 0.8 m, respectively. The range of salt gradient in the inner zones is such that the density is 1000–1045 kg/m^3 in the UCZ, 1045–1170 kg/m^3 in the NCZ, and 1170–1200 kg/m^3 in LCZ. Karakilcik and Dincer (2008) observed the temperature of the UCZ was a maximum of 35.0°C on August, a minimum of 10.4°C on January, and 27.9°C on May. Similarly, the temperature of the NCZ was observed as maximum as 44.8°C on August, a minimum of 13.9°C on January, and 37.9 °C on May, while the temperature of the LCZ is observed as maximum as 55.2°C on August, a minimum of 16.9°C on January, and 41.1°C on May. Velmurugan and Srithar (2008) determined that, by a blackened bottom in the pond, in LCZ, up to 40% of the total received solar energy can be absorbed. The temperature of this zone varies between 80 and 90°C. At the bottom of the pond, proper insulation is made to minimize losses. Suarez et al. (2010) presented a fully coupled two-dimensional, numerical model that evaluates the effects of double diffusive convection in the thermal performance and stability of a salt-gradient solar pond. The inclusion of circulation in the upper and lower convective zone clearly shows that erosion of the non-convective zone occurs. Model results showed that in a two-week period, the temperature in the bottom of the solar pond increased from 20°C to approximately 52°C and, even though the insulating layer is being eroded by double-diffusive convection, the solar pond remained stable. Singh et al. (2011) showed that, salinity-gradient solar ponds can collect and store solar heat at temperatures up to 80 °C, temperature difference in the range of 40–60 °C is available between the lower convective zone (LCZ) and the upper convective zone (UCZ).

The main aim of this work was to study the availability of construction of salinity gradient solar ponds (SGSPs) in Egypt, so can be used in thermal applications in agriculture and food processing.

The objectives of this research were as following:

• Study the temperature variations of the solar pond zones under Egyptian climate conditions.

• Study the density profiles for the solar pond.

- Evaluate the pond performance in collecting and storing solar energy.

MATERIALS AND METHODS

The experimental study was carried out during April, June and December 2010 at Faculty of Agriculture, Zagazig University, Sharkia Governorate, Egypt.

Materials

Experimental solar pond model

An insulated salinity-gradient solar pond model with a surface area of 1.5 m × 1.5 m and a depth of 1.44 m, as shown in Fig. 1, was constructed in Faculty of Agriculture, Zagazig University, Sharkia Governorate, Egypt (Latitude 30° 35′ N, Longitude 31° 31′ E). It was used to characterize the daily temperature variations and maximum temperature stored in UCZ, NCZ and LCZ. The bottom and the side-walls of the pond were plated with the iron-sheets in 2.5 mm thickness, and in between with a glass- wool of 10 cm thickness as the insulating layer. Inner and outer sides of the pond were painted with anti-corrosion paint then black paint. The solar pond was constructed on a steel base to 0.4 m above the ground and insulated with 10 cm thick glass wool.

Fig. 2 shows the experimental apparatus, which consists of a salt gradient small model pond that was made from iron-sheet, plastic water pipes, a thermocouple group T-type, control panel and weather station then plugged to computer.

Tap water

With density about of 1001 kg/m^3 at ambient temperature (Na = 0.041%, Cl = 0.032%) was considered zero concentration as initial conditions "control concentration".

Salt (NaCl)

Was the second main material for constructing and filling solar pond. Sodium chloride was used in this purpose due to it's properties and most widely available, cheap, easy solubility, good brine transparency, and easy maintenance without problems like algae growth.

Polystyrene

Thermoplastic substance, was used with 3.5 cm thickness and density of 6.886 kg/m^3 to obtain the concentration gradient initially by filling up the pond with several layers of salt solution, one on top of the other.

Methods

The solar pond model was studied under the following parameters:

Different climate conditions

The performance of the solar pond was studied under different climate conditions. Three experiments were carried out with three concentrations categories (Table 1) during April, June and December months.

Different ranges of salinity gradient

The three experiments were carried out under various weather conditions with 10 cm thickness of UCZ, 60 cm thickness of NCZ and 74 cm thickness of LCZ. These experiments were studied as shown in Table 1.

Filling the solar pond and establishing salt gradient

The top layer of UCZ had 0 % concentration (fresh water from tap) and vertical convection takes place due to effects of wind evaporation. The NCZ was 60 cm and it was split into four layers 15 cm thickness each. Salt gradient in NCZ was established by siphoning technique by using plastic water pipe with diameter of 1/2 inch and tank including the required concentration for each layer. The bottom layer (LCZ) has 74 cm thickness with uniform concentration of 6% in the first experiment, 10% in the second experiment, and 15% in the third experiment, as mentioned in Table 1.

For flow in the water pipe which used, the Reynolds number is generally defined as:

$$Re = \frac{\rho V D}{\mu} = \frac{V D}{\upsilon} = \frac{Q D}{\upsilon A} \qquad (1)$$

where:

D : The hydraulic diameter of the pipe (m).

Q : The volumetric flow rate (m^3/s).

A : The pipe cross-sectional area (m^2).

V : The mean velocity of the solution passes in pipe (m/s).

μ : The dynamic viscosity of the solution (Pa.s or N.s/m^2 or kg/m.s).

υ : The kinematic viscosity of the solution ($\upsilon = \mu / \rho$) (m^2/s).

ρ - The density of the solution (kg/m^3).

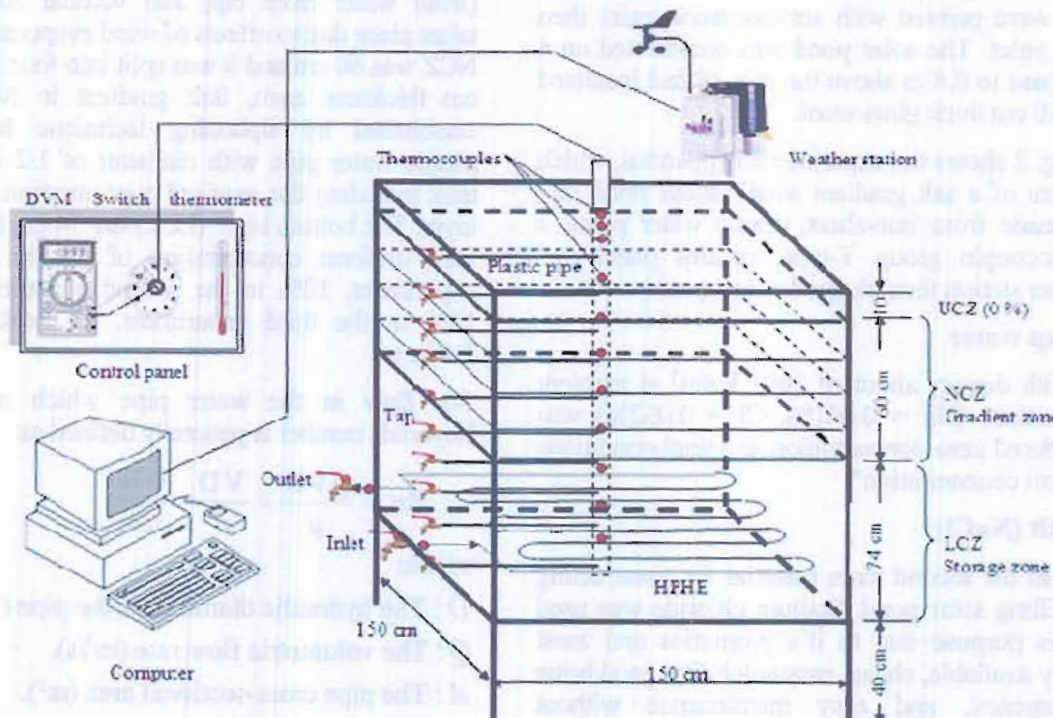Fig.1. A photo of the experimental model of a solar pond

Fig.2. A schematic view of the experimental apparatus for the solar pond model

Table 1. The distributions of salinity in the pond zones

Pond Zone	Pond zone thickness (cm)		Salinity (%)			
			Control	1st Exp.	2nd Exp.	3th Exp.
UCZ	10		0	0	0	0
NCZ	60	15	0	2	2	2
		15	0	3	4	5
		15	0	4	6	8
		15	0	5	8	12
LCZ	74		0	6	10	15

Measurements

Meteorological conditions (weather conditions)

Ambient temperature ($^{\circ}$C) and solar radiation intensity (in W/m^2) incident on the horizontal surface was measured by using a WatchDog weather station model of 900-ET with an accuracy of ±5%, ranging between 1-1250 W/m^2 of the output reading for solar radiation intensity and accuracy of ± 0.7°C, and ranging between -30 to 100°C of the output reading for temperature.

Density

Densities through the inner zones of the pond model in different pond layers were measured by using the method of weighing a certain volume for samples taken from different depths of the different layers of the pond. Samples of the saline water was extracted from different depths of the pond using simple gravity assisted siphoning technique by plastic water pipes and taps distributed on the side wall of solar pond model spaced at 5, 17.5, 32.5, 47.5, 62.5, 77.5, 92.5, 107.5, 122.5, 137 cm from the surface to the bottom of solar pond.

Viscosity

Viscosity coefficients for all concentrations in the inner zones of the pond model in different layers were determined by falling ball method and Stokes' law. A graph of v against r^2 was plotted and the viscosity of sample (μ) was determined from:

$$\mu = \frac{2gr^2(\rho-\sigma)}{9v} \qquad (2)$$

Where: ρ is the density of ball, σ is the density of sample (g= 9.81 m/s^2).

Temperature

Within the whole experiments, temperatures through the inner zones of the pond model were measured by using 12 temperature sensors (copper-constantan thermocouples type "T") were taken at different locations along the centered inner of the pond, as indicated in Fig. 2, by using T-type thermocouples. These thermocouples were spaced at 2, 6, 10, 25, 40, 55, 70, 85, 100, 115, 130, and 142 cm interval from the surface of the pond to the bottom. The temperature distributions at these regions were recorded at 1 hour time interval during day times from 9:00 at the morning to 16:00 at the afternoon.

Performance analysis of the solar pond

By knowing latitude of location and hourly global radiation measured horizontally using WatchDog weather station, a mathematical model to calculate the variation of the solar radiation flux (W/m^2) as it penetrates through the horizontal solar pond was investigated, as the following expressions (Duffie and Beckman, 1991):

1. Calculation of solar declination angle (δ) :

$$\delta = 23.45 \times \sin\left((284+n) \times \frac{360}{365}\right), \quad n: \text{ number of}$$

days in year   (3)

2. Calculation of solar time (t):

$$B = (n-1)\frac{360}{365} \qquad (4)$$

$$E = 229.2 \times (0.000075 + 0.001868\cos B - 0.03277\sin B$$
$$- 0.014615\cos 2B - 0.04089\sin 2B) \qquad (5)$$

solar time (t) = standard time − 4 (L$_{st}$ − L$_{loc}$) + E   (6)

Where, L_{st} is the standard meridian for the local time zone, 30° for Egypt, L_{loc} is longitude of the location in equation in degrees west, 31.52° for the present work and B, E are constants.

3- Calculation of solar hour angle (ω):

$$\omega = 15(t - 12) \qquad (7)$$

4- Calculation of latitude angle (φ):

for present work, $\varphi = 30° \ 35^\backslash = 30.58°$

5- Calculation of angle of incidence (θ_z) for beam and diffuse radiation:

For beam radiation,

$$\theta_{zb} = \cos^{-1}(\cos\varphi\cos\delta\cos\omega + \sin\varphi\sin\delta) \quad (8)$$

For diffuse radiation, $\theta_{zd} = 60°$, when diffuse radiation is incident on it presents some difficulty because the radiation comes from many directions. The usual practice is to assume that the diffuse radiation is equivalent to beam radiation coming at an angle of incidence of 60° due to reflection is small and ranges from 2% to 6%.

6- Calculation of angle of refraction in water (θ_w) for beam and diffuse radiation:

For beam radiation, $\theta_{wb} = \sin^{-1}\left(\dfrac{\sin\theta_{zb}}{1.33}\right)$ (9)

For diffuse radiation, $\theta_{wd} = \sin^{-1}\left(\dfrac{\sin 60°}{1.33}\right) = 40.63°$ (10)

7- Calculation of reflectivity (r):

For beam radiation,

$$r_b = \frac{1}{2} \times \left(\frac{\sin^2(\theta_{wb} - \theta_{zb})}{\sin^2(\theta_{wb} + \theta_{zb})} + \frac{\tan^2(\theta_{wb} - \theta_{zb})}{\tan^2(\theta_{wb} + \theta_{zb})} \right) \quad (11)$$

For diffuse radiation,

$$r_d = \frac{1}{2} \times \left(\frac{\sin^2(40.63 - 60)}{\sin^2(40.63 + 60)} + \frac{\tan^2(40.63 - 60)}{\tan^2(40.63 + 60)} \right) = 0.059 \quad (12)$$

8- Calculation of transmissivity based on reflectance (τ_r):

For beam radiation, $\tau_r = 1 - r_b$ (13)

For diffuse radiation, $\tau_d = 1 - r_d$ (14)

9- Calculation of transmissivity based on absorption (τ_a):

For beam radiation, $\tau_{ab} = 0.36 - 0.08 \ln\left(\dfrac{z}{\cos\theta_{wb}}\right)$ (15)

For diffuse radiation, $\tau_{ad} = 0.36 - 0.08 \ln\left(\dfrac{z}{\cos 40.63°}\right)$ (16)

Where: z = the depth of water inside the pond, in meters.

10- Calculation of extraterrestrial radiation on the horizontal SGSP (I_o):

The solar radiation outside the atmosphere, that is, the hourly extraterrestrial radiation incident on horizontal plane for a period between hour angles ω_1 and ω_2 which define an hour (where ω_2 is the greater) can be written by the following way:

$$I_o = \frac{12 \times 3600}{\pi} I_{sc}\left(1 + 0.033\cos\frac{360n}{365}\right) \qquad (17)$$
$$\times \left(\cos\varphi\cos\delta(\sin\omega_2 - \sin\omega_1) + \frac{\pi(\omega_2 - \omega_1)}{180}\sin\varphi\sin\delta \right)$$

Where: (I_{sc}) is the solar constant, the mean radiation flux density outside of earth's atmosphere, is 1367 W/m^2 (with $\pm$ 1%), with most of the radiation in a wavelength range of 0.3 to 3 µm.

11- Calculation of terrestrial solar radiation for beam (I_b) and diffuse radiation (I_d):

The correlation between hourly diffuse and global radiation showed by (Muneer and Sahili, 1984) can be expressed by the following ways:

$$\frac{I_d}{I_h} = \begin{cases} 0.95 & \text{for } k_T \le 0.175 \\ 0.9698 + 0.4353k_T - 3.4499k_T^2 & \text{,for } 0.175 \le k_T \le 0.775 \\ \quad + 2.1888k_T^3 & \\ 0.26 & \text{for } k_T > 0.775 \end{cases} \quad (18)$$

Where:

(I_h) is the total solar radiation on a horizontal surface from available pyranometer measurements (measured by WatchDog weather station, W/m^2).

While:

(k_T) is the hourly clearness index, where:

$$k_T = \frac{\text{Total solar radiation on a horizontal surface}}{\text{Extraterrestrial solar radiation on that surface}} = \frac{I_h}{I_o} = \text{Clearness index}$$

12- The beam radiation can be calculated by:

$$I_b = I_h - I_d \qquad (19)$$

13- Calculation of the flux reflected from water surface (I_{air}) and the flux entering water (I_{water}) :

The flux reflected from surface of the solar pond can be expressed as:

$$I_{air} = I_b r_b + I_d r_d , \qquad W/m^2 \qquad (20)$$

Therefore, flux entering water can be expressed as: $I_{water} = I_h - I_{air} , \qquad W/m^2 \qquad (21)$

14- Calculation of the solar flux as it penetrates through different depths of pond (I_z) :

Solar flux (I) at a depth of (z) from the pond surface can be expressed as:

$$I_z = I_b \tau_{rb} (\tau_{ab})_z + I_d \tau_{rd} (\tau_{ad})_z , \qquad W/m^2 \qquad (22)$$

3.6. Thermal efficiency of the solar pond:

$$\text{Thermal efficiency of the solar pond} = \frac{T_{LCZ} - T_a}{T_{LCZ}} \times 100 \quad (23)$$

Where:

T_{LCZ} : temperature stored in LCZ, °C.

T_a : ambient temperature, °C.

Collection efficiency of the solar energy

The energy collection efficiency of the solar pond was calculated as the following equation:

$$\text{Collection efficiency of the solar pond} = \frac{I_z}{I_h} \times 100 \quad (24)$$

Where:

I_Z : the flux at specified depth in the pond (z), W/m^2.

I_h : the measured beam radiation on the horizontal pond surface, W/m^2.

RESULTS AND DISCUSSION

The discussion will cover the obtained results under the following heads:

Effect of Concentration on Viscosity and Reynolds Number

Because the temperature of fluid maintained at the ambient temperature (25°C) under atmosphere pressure within all tests, the only cause of a change in total mass is a change in fluid density due to increasing of concentration. As shown in Fig. 3, the viscosity coefficients were considered as an increasing function of the solute concentration but Reynolds number was considered as a decreasing function of the solute concentration. It was shown that, when the solute concentration increased from 0 to 12 %, the viscosity coefficient increased from 0.0452 to 0.1883 Pa.s, on the other side, Reynolds number decreased from 156 to 41. This means that, filling of the solar pond was under laminar flow within whole experiments, this proved that, there was no mixing of the pond layers with each other during the filling process.

The Density Profile of the Solar Pond

Density values were obtained as shown in Fig. 4, generally it has been found that, the density profiles initially looks like stair steps, then it starts to turn to a shape like the SGSP density profile (The transient behavior of the salinity gradient solar pond) after the five days. The range of density of salt gradient in the inner zones for initial conditions was 998-1014 kg/m³ in the UCZ, and 1012-1050 kg/m³ in the NCZ, and 1036-1051 kg/m³ in LCZ for 1st exp., 1000-1018 kg/m³ in the UCZ, and 1012-1075 kg/m³ in the NCZ, 1066-1086 kg/m³ in LCZ for 2nd exp. and 1000-1032 kg/m³ in the UCZ, and 1012-1106 kg/m³ in the NCZ, 1100-1125 kg/m³ in LCZ for 3rd exp.

The Temperature Variations for the Solar Pond Zones

Fig. 5 shows the temperature development of the pond zones for the three experiments with ambient temperature in array shape. In general, with an overview, it was found that, in a column and at the same weather conditions, the temperature stored in the layers of the pond increased gradually from the first experiment until the third, the highest in the concentration of salinity. While in a row temperatures stored in the layers of the pond increased in summer more than during spring than during winter, all over
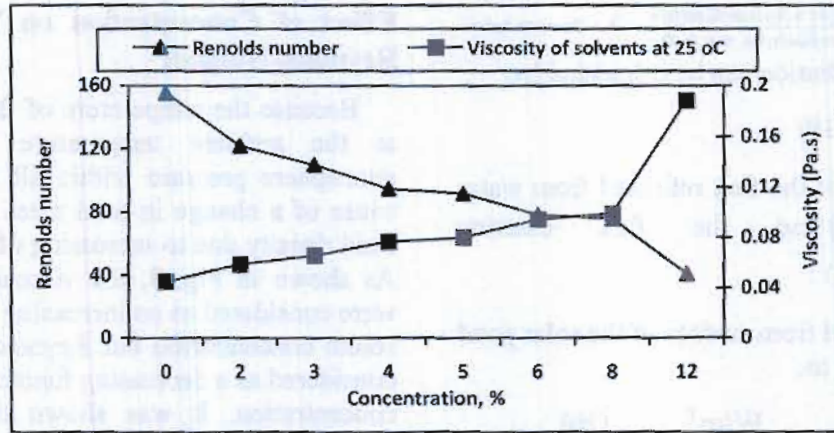
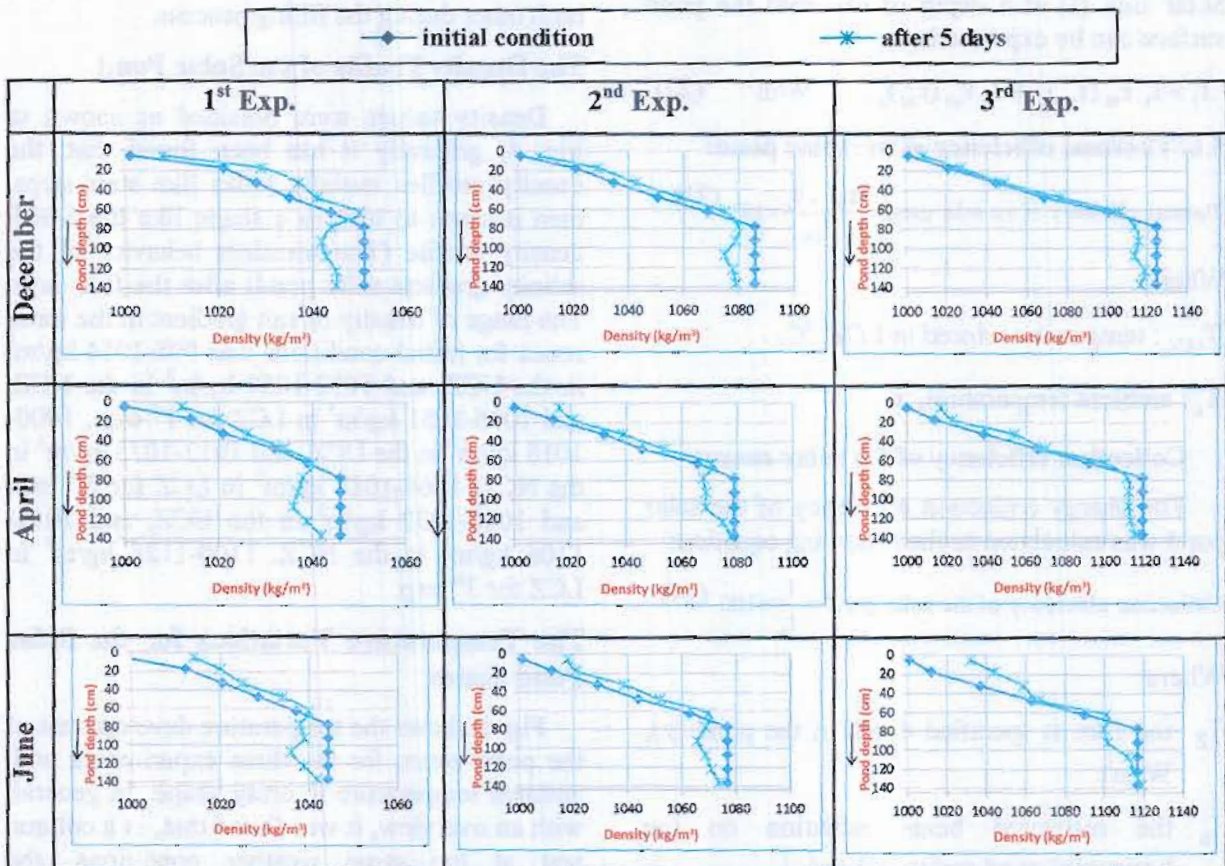Fig.3. Viscosity coefficients and Reynolds number at the various concentrations

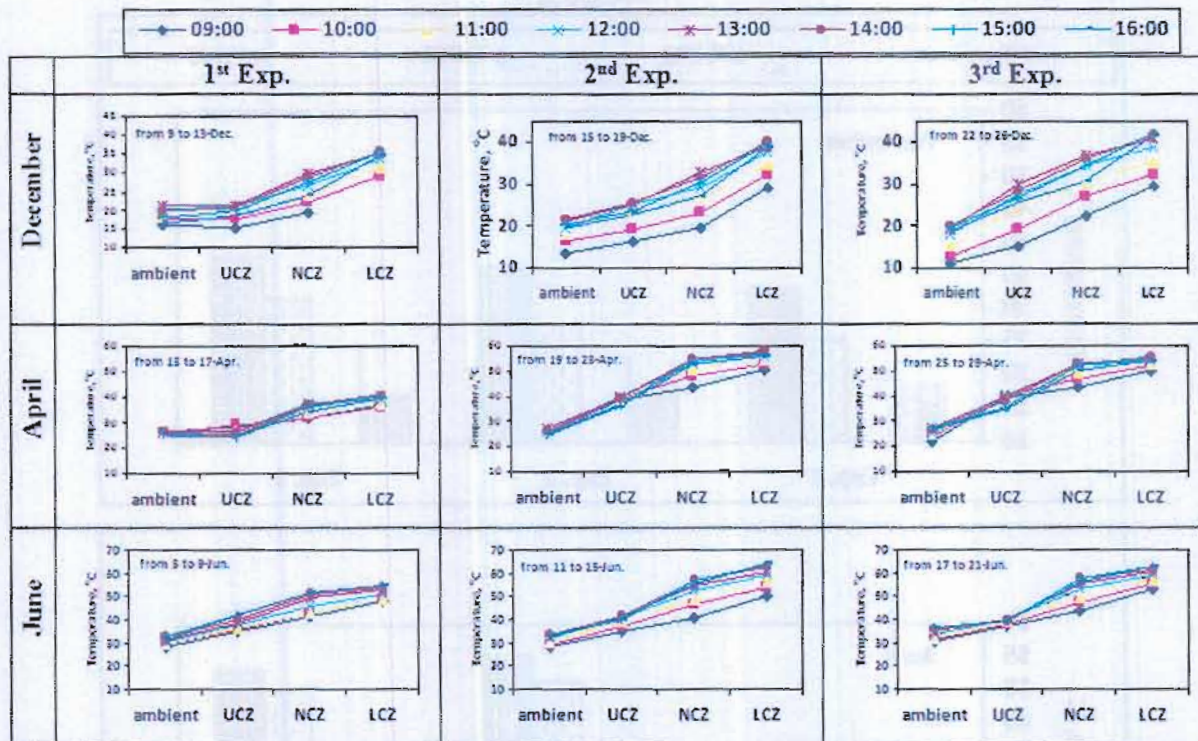Fig.4. Density profiles of the solar pond for each experiment

Fig. 5. Diagram of temperature vzriations of the pond zones for each experiment during daytimes

the daylight hours from 9:00 am to 16:00 pm. For 1st exp., the maximum values of temperature stored in LCZ were 35.8, 40.6 and 54.7°C during December, April and June, respectively. For 2nd exp., the maximum values of temperature stored in LCZ were 40.2, 58.1 and 63.9°C during December, April and June, respectively. For 3rd exp., the maximum values of temperature stored in LCZ were 42.3, 55.5 and 62.6°C during December, April and June, respectively. Variations in the stored temperatures were due to the salinity differences.

Thermal Efficiency of the Solar Pond

Fig. 6 shows the overall average temperature variations during winter, spring and summer seasons. During winter season (December), in the pond bottom, it can be noticed a good solar heating effect. In the central gradient region, although the thermal behaviors of the pond during the winter can be attributed to cold ambient air temperatures as well as to a relatively low level of the incident solar radiation, in a comparison with spring and summer seasons (it's averaged value is estimated to be only 230 W/m² throughout this season). The temperature stored in LCZ reaches approximately 32.9°C (about 43.7% of thermal efficiency), 36.5°C (about 48.5% thermal efficiency), and 37.9°C (about 55.5% thermal efficiency), for 1st, 2nd and 3rd experiments, respectively, while the averaged ambient air temperature was 18.5, 18.8 and 16.9°C for 1st, 2nd and 3rd experiments, respectively.

For the spring season i.e. during the month of April, both solar radiation level and ambient air temperature clearly increased. The average of recorded value of solar radiation was about 680 W/m². Such an increase of the solar radiation has, of course, a direct effect on the temperature profile. The temperature stored in LCZ reaches approximately 38.9°C (about 32.9% of thermal efficiency), 55.3°C (about 53.3 % thermal efficiency), and 53.5°C (about 52.6% thermal efficiency), for 1st, 2nd and 3rd experiments, respectively, while the averaged ambient air temperature was 26.1, 25.9 and 25.4°C for 1st, 2nd and 3rd experiments, respectively.
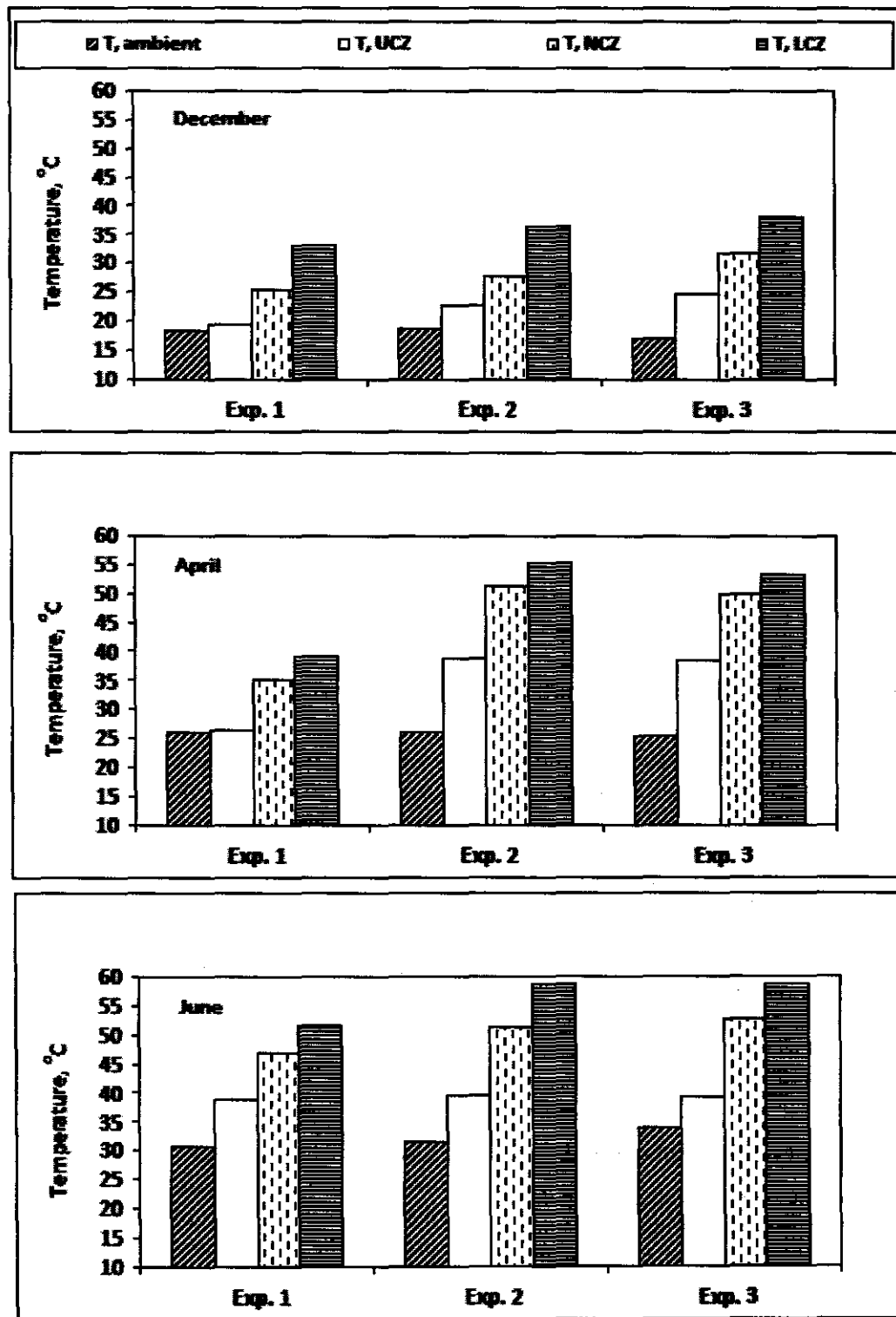
Fig. 6. The overall average temperature of the pond zones

For the summer season i.e. during the month of June, both solar radiation level and ambient air temperature clearly increased. The averaged incident solar radiation was estimated to be nearly 740 W/m^2. Also, it should be noted that during this season, extreme values of these weather variables have been observed. The corresponding increase of saline temperature appears very important.The temperature stored in LCZ reaches approximately 51.7°C (about 40.7% of thermal efficiency), 58.6°C (about 46.3 % thermal efficiency), and 58.6°C (about 42.6% thermal efficiency), for 1st, 2nd and 3rd experiments, respectively, while the averaged ambient air temperature was 30.6, 31.5 and 33.8°C for 1st, 2nd and 3rd experiments, respectively.

Fig. 7 shows the thermal gain of the solar pond during December, April and June months. In general, it was observed in the third experiment, that the thermal gain of the solar pond reach a maximum in winter, as Egypt enjoys clear sky and warm atmosphere and the sun bright in the winter, although under solar radiation in winter lower than it in spring and summer. Such behavior shows, however, that a SGSP may operate under relatively high temperature range, condition that can be advantageous for some thermal applications.

Relationship between Temperature of LCZ and Ambient Temperature

Solar ponds are affected by the atmospheric conditions above the pond, so LCZ temperatures plotted versus the ambient temperatures under Egyptian seasonal solar radiation for the experiment (3) with difference of salinity is 15% of NaCl between the surface and the bottom of the pond as shown in Fig. 8. As external temperature is increased, the model shows a drastic response within the LCZ temperature. The results are linear within the range of expected values with a slope of 1.4014, 0.8584 and 1.6307 for December, April and June respectively.

Collection Efficiency of Solar Energy in the Solar Pond

The main results of calculation reflection and absorption of solar radiation in the solar pond obtained from the mathematical analysis for simulation of estimating the variation of solar flux as it penetrates through the solar pond. The results show that, about 94.3% of the incident energy on surface of the pond entering the water and 5.7% of the incident energy was reflected to the surroundings. The results shown in Fig. 9 (for a location in Zagazig), show the mean collection efficiency for the investigated solar pond. It was noted that, the collection efficiency was 49.3 % for UCZ layer, 34.6% for NCZ layer and 29.2% for LCZ layer. Fig. 8 can be also, used for approximately estimating solar pond efficiency for solar energy collection in locations having similar annual values of ambient temperature and global radiation.

Conclusion

On December, The temperature stored in LCZ reaches approximately 32.9°C for the first experiment, 36.5°C, for the second experiment and 37.9°C, for the third experiment, where the averaged ambient air temperature was approximately only 18.1°C for the entire season and the averaged value of solar radiation intensity about 230 W/m^2. On April, both solar radiation level and ambient air temperature have clearly increased, the respective averaged values were 680 W/m^2 and 25.8°C. For the first experiment, the temperature stored in LCZ reached approximately 38.9°C, 55.3°C, for the second experiment and 53.5°C, for the third experiment. The development of LCZ temperature for the summer season during which, the averaged ambient air temperature and incident solar radiation were estimated to be 32°C and nearly 740 W/m^2. For the first experiment, the temperature stored in LCZ reached approximately 51.7°C, 58.6°C, for the second experiment and 58.8°C for the third experiment.

Based on the obtained results, it is recommended to use the concentrations of salt as in the 3rd experiment to get high stored temperature in the bottom of the solar pond. The temperature of each layer of the inner zones depends on the incident radiation, zone thicknesses and overall heat losses. The results showed, about 94.3% of the incident energy on surface of the pond entering the water and 5.7% of the incident energy was reflected to the surroundings. The mean collection efficiency of solar radiation for the investigated solar pond was about 49.3% for UCZ layer, 34.6% for NCZ layer and 29.2% for LCZ layer. This means that, solar ponds can be applied in Egypt to get a good thermal performance, and used in many thermal applications in the field of agriculture, water heating, water desalination and food processes.
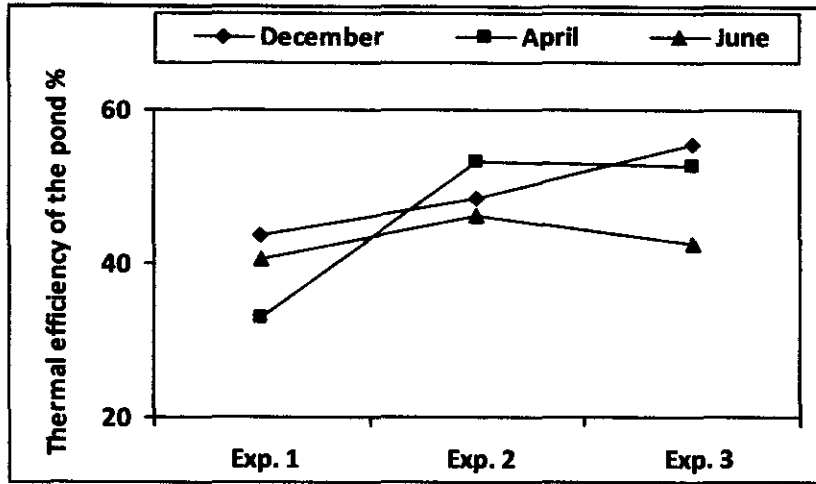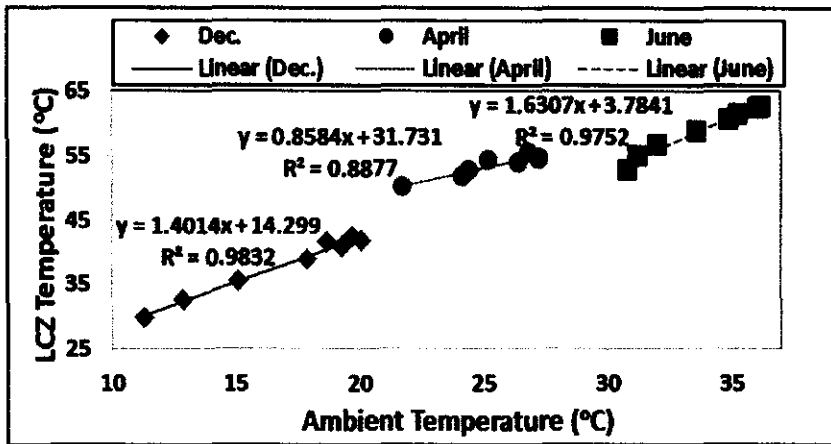
Fig.7. The thermal efficiency of solar the pond

Fig.8. Thermal gradient in LCZ as a function of T-ambient above the pond for 3rd Exp.
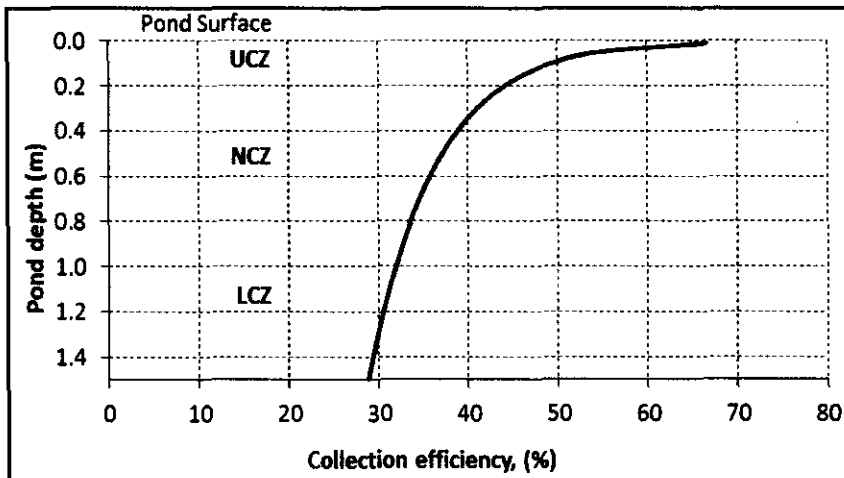

Fig. 9. Collection efficiency of the solar pond

REFERENCES

Akbarzadeh, A., J. Andrews and P. Golding (2005). Solar pond technologies: a review and future directions. Advances in Solar Energy, EARTHSCAN (Chapter 7).

Angeli, C. and E. Leonardi (2004). A one-dimensional numerical study of the salt diffusion in a salinity-gradient solar pond. International Journal of Heat and Mass Transfer, 47: 1–10.

Dah, M.M.O., M. Ouni, A. Guizani and A. Belghith (2005). Study of temperature and salinity profiles development of solar pond in laboratory. Desalination, 183: 179–185.

Duffie, J.A. and W.A. Beckman (1991). Solar Engineering of Thermal Processes, 2nd ed. New York "USA": A Wiley-Interscience. John Wiley and Sons, Inc.

Jaefarzadeh, M.R. (2004). Thermal behavior of a small salinity-gradient solar pond with wall shading effect, Sol. Energy, 77: 281–290.

Karakilcik, M., I. Dincer and M.A. Rosen (2006). Performance investigation of a solar pond. Applied Thermal Engineering, 26: 727–735.

Karakilcik, M. and I. Dincer (2008). Exergetic performance analysis of a solar pond. International Journal of Thermal Sciences, 47: 93–102.

Kurt, H., F. Halici and A. Korhan Binark (2000). Solar pond conception-experimental and theoretical studies, Energy Convers. Manage, 41 (9): 939–951.

Muneer, T.M.M. and H.K. Sahili (1984). Correlation between hourly, diffuse and global radiation for New Delhi. Energy Conservation and Management, 24: 265-267.

Singh, R., S. Tundee and A. Akbarzadeh (2011). Electric power generation from solar pond using combined thermosyphon and thermoelectric modules. Solar Energy, 85: 371–378.

Suarez, F., S.W. Tyler and A.E. Childress (2010). A fully coupled, transient double-diffusive convective model for salt-gradient solar ponds. Inter. Journal of Heat and Mass Transfer, 53:1718–1730.

Velmurugan, V. and K. Srithar (2008). Prospects and scopes of solar pond: A detailed review. Renewable and Sustainable Energy Reviews, 12: 2253–2263.

تقييم أداء نموذج بركة شمسية متدرجة الملوحة تحت ظروف الإشعاع الشمسي فى مصر

وسـام السيد عبد الحميد عبد الله ـ محمد قدري عبد الوهاب
محـب محمد أنيس الشربـاصى ـ محمود مصطفى على على

قسـم الهندسة الزراعيـة ـ كليـة الزراعـة ـ جامعة الزقازيق ـ مصر

تعتبر البرك الشمسية نظاماً بسيطاً وجيداً لتجميع وتخزين الطاقة الشمسية على نطاق واسع. يقدم هذا البحث نموذجاً مبسطاً لبركة شمسية متدرجة الملوحة بمساحة سطحية (1,5×1,5)م²، وعمق 1,44 م معزولة حرارياً من الجوانب ومن أسفل. تم إنشاء وتجريب هذه البركة في كلية الزراعة ـ جامعة الزقازيق ـ محافظة الشرقية ـ مصر (خط طول 31/ 31° شرقاً ، خط عرض 30 /35 ° شمالاً) بهدف تحسين كفاءة البركة الشمسية للوصول إلى أقصى درجة حرارة يمكن تخزينها تحت الظروف المناخية المصرية خلال عام 2010 م. تم ملء البركة الشمسية بتركيزات مختلفة من الماء المذاب به ملح كلوريد الصوديوم فى ثلاثة طبقات رئيسية هى: طبقة الحمل السطحية (UCZ) وسمكها 10سم وطبقة اللاحمل الوسطية (NCZ) وسمكها 60 سم مقسمة إلى أربعة تركيزات للملح موزعة على أربعة طبقات صغيرة متساوية السمك (15سم) وطبقة الحمل السفلية (LCZ) وسمكها 74 سم. وكان فرق تركيز الملوحة بين طبقتي الحمل السطحية والسفلية 6% للتجربة الأولى ، 10٪ للتجربة الثانية ، 15٪ للتجربة الثالثة. تم استخدام 12 ازدواج حراري من النوع (T) موزعة فى وسط البركة فى الإتجاه الرأسي من أعلى إلى باطن البركة وذلك لقياس تغيرات درجات الحرارة خلال ساعات النهار ، واعتبرت درجات الحرارة المقاسة مؤشراً لإنتقال الحرارة إلى باطن البركة لتقييم أداء البركة الشمسية فى تجميع وتخزين الطاقة الشمسية فى صورة طاقة حرارية. تم تصميم نموذج رياضي بالمعادلات والصيغ الرياضية يحاكى إنتقال وتدفق الإشعاع الشمسى إلى باطن البركة لقياس كفاءة البركة الشمسية فى تجميع الطاقة الشمسية وتخزينها فى الطبقة السفلية للبركة الشمسية. كانت أفضل النتائج المتحصل عليها في التجربـة الثالثة (تركيز الملوحة للطبقة السطحية صفر ٪، تدرجات الملوحة للطبقة الوسطي 2 ، 5 ، 8 و 12٪ و تركيز الملوحة للطبقة السفلية 15٪)؛ فقد وصلت درجات الحرارة إلى أعلى قيم تم تخزينها كما يلى: في شهر أبريل كانت درجات الحرارة المخزنة هي: (38,3 ، 49,9 و 53,5) مْ للطبقات السطحية والوسطي والسفلي على الترتيب. في شهر يونيو كانت درجات الحرارة المخزنة هي: (39,1 ، 52,6 و 58,8)مْ عند نفس الطبقات. وأيضا خلال شهر ديسمبر كانت درجات الحرارة المخزنة هي: (24,7 ، 31,8 و 37,9) مْ تحت نفس الطبقات. كذلك أوضحت النتائج أن كفاءة تجميع الطاقة الشمسية بنظام البرك الشمسية على عمق (1,44م) تحت ظروف الإشعاع الشمسى فى مصر حوالى (29,2٪) مما يجعل تطبيق تكنيك البرك الشمسية فى مصر فكرة جيدة للحصول على أداء حراري جيد وكذلك استخدامها في كثير من التطبيقات الحرارية فى مجال الزراعة مثل تدفئة الصوب الزراعية، تسخين المياه، تحلية المياه، عمليات التجفيف، عمليات التبريد وفي عمليات التصنيع الغذائى.